Temperature and salinity variability recorded by *Cladocora caespitosa*: a multi-proxy analysis of a shallow-water Mediterranean coral

Eli Mitchell-Larson

Advisor: Mark Pagani

Second Reader: Zhengrong Wang

May 1st, 2013

A Senior Essay presented to the faculty of the Department of Geology and Geophysics, Yale University, in partial fulfillment of the Bachelor's Degree.

Abstract

Shallow water Mediterranean corals present a high-resolution geochemical archive for paleoclimate reconstruction in the Mediterranean basin. However, conventional proxies such as the oxygen isotopic composition of carbonate may reflect multiple environmental parameters and are often complicated by species-specific biological effects. Carbonate clumped isotope thermometry (Δ_{47}) is a temperature proxy that may record absolute temperature, thereby bypassing these problems. Magnesium isotopic composition ($\delta^{26}Mg$) may also serve as a valuable temperature proxy since the carbonate-seawater fractionation factor ($\Delta^{26}Mg$) has been shown to be temperature dependent. This study explores the variability of clumped isotopes and magnesium isotopes in biogenic aragonite from modern environmental and aquaria-cultured specimens of *Cladocora caespitosa*, a shallow water scleractinian coral that is spatially abundant throughout the Mediterranean and extant extending back to the early Pleistocene. Δ_{47} and $\delta^{26}Mg$ values are constrained against *in situ* and other temperature data, as well as against more traditional geochemical proxies including $\delta^{18}O$ and the ratios of substituted trace metal cations in the aragonite lattice. Results show clear seasonal cycles in $\delta^{18}O$ and Sr/Ca that inversely covary with $\delta^{13}C$. Data from clumped isotopes measurements suggest warm temperatures during coral $\delta^{18}O$ and Sr/Ca maxima, an unexpected result if $\delta^{18}O$ is influenced primarily by temperature and not $\delta^{18}O_{water}$. This discrepancy could be resolved if clumped isotope were reduced through additional replicates or reproducibility were improved with additional cleaning steps to ensure that all organic compounds are removed from the skeleton. Regardless, application of clumped isotopes to this species remains optimistic given that the Δ_{47}-derived temperatures fall within the expected range of temperature variability for the site, do not exhibit the biologically-mediated offset observed in Δ_{47} data from some other coral species, and produce more realistic temperatures in *Cladocora caespitosa* than do existing equations relating $\delta^{18}O$ of aragonite to temperature even when $\delta^{18}O_{seawater}$ is known. $\delta^{26}Mg$ values from the aquaria-cultured specimens suggest some temperature dependence of $\Delta^{26}Mg$ for *Cladocora caespitosa*, though data from additional environmental samples with well-constrained growth temperatures are needed to build a robust calibration.

1. Introduction

1.1 The Mediterranean Basin

The Mediterranean is a complex, semi-enclosed basin that has the capacity for profound climatological and geochemical variability over time (Bethoux et al., 1999). The paleoclimate history of the Mediterranean is of great interest, particularly as it can be conceived of as a miniature ocean complete with evidence for past responses of deep water formation and thermohaline circulation to climate changes (Cacho et al., 2000; Bethoux et al., 1999). Mediterranean seasonality is complicated by the fact that the regional climate is alternately influenced by descending Hadley cell convection in the summer and prevailing Westerlies in the winter (Bolle et al., 2003). This is partially responsible for the relatively large seasonal sea surface temperature (SST) variability of 10-21 °C and 15-26 °C in the Western and Eastern Mediterranean respectively (Artegiani et al., 1997; Rohling et al., 2009). The Mediterranean typically experiences a warm, dry summer followed by a mild, rainy winter with evaporative flux often exceeding precipitation. As a result of this surplus evaporation, sea surface salinity (SSS) ranges from roughly Atlantic values in the far West to much higher values in the East, for example a winter salinity of 38.7 psu in the Adriatic (Stenni et al. 1995). However, many records of important climatic parameters like SST and SSS are often sparse, short in duration, or non-continuous in the Mediterranean (Montagna 2006). Continuous and high resolution records of these climate conditions in both the modern and the paleoclimate record are highly desirable to improve our understanding of Mediterranean climate dynamics.

1.2 Reconstructing climate from corals

Among the sources of biogenic carbonates used for reconstructing paleoclimate conditions corals are promising and offer both advantages and challenges to coherent intepretation. Coral colonies are made up of polyps which continually secrete a calcerous skeleton, typically composed primarily of aragonite, a less stable polymorph of calcite which nonetheless persists plentifully in the fossil record (Correge 2005). These aragonite skeletons incorporate stable isotopes of carbon and oxygen, as well as substituted trace metal cations, as a function of both the physical and chemical qualities of ambient seawater and biologically modulated offsets called 'vital effects'. Massive corals are resistant to erosion and mechanical breakage and have been known to reach ages of 700-1000 years (Burr et al., 1998). Reconstructions from such corals have been particularly valuable in the tropics where multi-century instrumental climate records are sparse, incomplete, or non-existent (Grottoli 2001). Because coral growth rates are fast compared with other biogenic and abiogenic carbonate sources, ranging from a few mm to upwards of 2 cm per year, they are among the best records for high-resolution, sub-annual analysis using geochemical tracers (Correge 2005). Reef building corals of the genus scleractinia are the most commonly studied because they are widely distributed around the world and typically live in shallow water, thereby recording conditions in the upper thermocline (Correge 2005). Scleractinia can also be used to constrain past sea level by assuming fossil reef platforms grew at similar depth to extant modern reefs of the same species (Lambeck et al., 2004; Peirano et al., 2004). Though corals avoid the age modeling issues imposed by bioturbation in sediment cores due to their tough stony skeletons, their variable growth rates can alter the processes of incorporation of isotopes and ions into their aragonitic skeletons, complications which are reviewed below for specific SST and SSS proxies.

The least analytically complex proxy for interpreting coral records is the correlation of annual growth rate with climatic parameters. Just as dendrochronology analyzes the growth rings in trees to understand variability in terrestrial environments, sclerochronology is used to track

Figure 1 - MicroCT scan of a *Cladocora caespitosa* corallite from Mljet, Croatia showing alternating HD and LD bands. Two bands are typically deposited per year, serving as a useful age constraint to guide sub-sampling in sub-annual analysis.

growth in corals through the alternation of high density (HD) and low density (LD) secretion bands (Peirano et al., 2004; Correge 2005). Growth rates have been shown to correlate with temperature (Peirano et al., 2004). Figure 1 shows an x-ray cross-section of a coral from this study that shows aragonite density as a function of luminosity. Because most corals deposit one HD and one LD band each year, one year of growth can be defined as the distance between two successive HD band peaks (Peirano et al., 2004).

1.2.1 $\delta^{18}O$

Following early work in geochemical paleothermometry that established the temperature dependence of oxygen isotopic fractionation in carbonates (Urey et al., 1951; Epstein et al.,

1953), coral skeletons became an early candidate for the $\delta^{18}O$ temperature proxy. In marine biogenic carbonates, the interpretation of $\delta^{18}O$ values as a temperature signal is complicated by the need to deconvolve the influence of changing global ice volume in the paleoclimate record (Billups and Schrag 2002), account for local evaporation and freshwater influx effects (Craig 1961), and understand species-specific vital effects, all of which blur the clarity of this paleothermometer. While most molluscs and foraminifera tests secrete calcareous skeletons carrying $\delta^{18}O$ signatures identical to inorganic carbonate precipitated at the same temperature (Epstein et al., 1953), calcification in corals was shown early on to be out of isotopic equilibrium with ambient seawater (Epstein et al., 1951). Weber and Woodhead (1972) showed that despite this disequilibrium, $\delta^{18}O$ versus temperature curves for many coral genera were parallel to the inorganic precipitation curve and offset toward lower $^{18}O/^{16}O$ ratios. This isotopic disequilibrium stems largely from kinetic isotope effects during CO_2 hydration and hydroxylation which deplete $^{18}O/^{16}O$ as much as 4 ‰ as CO_2 reacts to form HCO_3^- (McConnaughey et al., 1989a). This negative offset is modulated by the speed of skeletogenesis with high speeds favoring strong kinetic effects. In zooxanthellate corals growth rate may depend on both temperature and the level of photosynthetic activity of the algal symbionts, therefore kinetic fractionation must be interpreted with care. The large calcification rates of corals are both a blessing and a curse. Due to their abundant annual secretion corals allow high-resolution reconstructions in regions with limited temperature records or a lack of alternative geologic archives as discussed above, but their fast growth rates can cause non-equilibrium isotopic effects induced in part by the algal symbionts. $\delta^{18}O$ can vary among fast and slow growing regions of skeleton in a single coral colony, or among multiple colonies growing contemporaneously and at the same site (McConnaughey 1989a; McConnaughey 1989b). In sites where both sea temperature and salinity

vary little throughout the year, $\delta^{18}O$ variability can nevertheless exceed what would be expected if the signal were driven only by temperature and water flux. For example Jamaican corals that experienced annual variability of ~4 °C and ~1 psu expressed a $\delta^{18}O$ range upwards of 4‰, likely as a result of vital effects (Keith and Weber 1965). Despite these difficulties with interpretation, $\delta^{18}O$ has been one of the most commonly studied and reported proxies for reconstructing SST and SSS from corals (Correge 2005).

1.2.2 Trace element ratios

Corals incorporate trace metal cations (e.g. Mg^{2+}, Sr^{2+}, Ba^{2+}, etc.) in their aragonitic skeletons ($CaCO_3$) as a function of both the ratio of that cation with Ca^{2+} in ambient seawater and a distribution coefficient between aragonite and seawater characteristic to that cation. This distribution coefficient has been shown to be temperature dependent for many trace metal cation systems (McIntire 1963; Beck et al., 1992). The most effective of these proxies in reproducing SST in corals is Sr/Ca (Correge 2005). Unlike the $^{18}O/^{16}O$ of seawater, a parameter which varies greatly both over geologic time with changing global ice volume and on short timescales in response to local evaporative or rainfall events, the ratios of many cations remain more or less constant on long timescales. It is believed that the Sr/Ca ratio of the world's oceans has held roughly constant for the past ~10^5 years (Beck et al., 1992), and that the residence time of Ca^{2+} is ~1.1 x 10^6 years (Mitsuguchi et al, 1996). This makes the Sr/Ca paleothermometer theoretically 'cleaner' than $\delta^{18}O$ since fewer assumptions about past ocean chemistry need to be made. However, subtle changes in Sr/Ca and other trace element ratios over space and time have the potential to influence SST estimates (de Villiers et al., 1994). Like $\delta^{18}O$ there is no universal

calibration for Sr/Ca as species-specific effects appear to influence the uptake of Sr^{2+}, however most calibration equations hover around an average temperature dependence of -0.06 mmol/mol $°C^{-1}$ (Correge 2005). The main advantage of Sr/Ca as a temperature proxy is that an *in situ* calibration in the modern can be applied more confidently toward reconstructing paleoclimate conditions than can $\delta^{18}O$. By coupling the two proxies Sr/Ca filters out the effect of temperature from the $\delta^{18}O$ signal, allowing the interpretation of $\delta^{18}O$ as a recorder of SSS. Mg/Ca ratios are also potentially useful given the 13 million year residence time for Mg^{2+} (Mitsuguchi et al., 1996), however the mechanism for uptake and incorporation of Mg^{2+} into coral aragonite is poorly understood (Silenzi at al., 2005). The first highly successful demonstration of Mg/Ca thermometry in corals was performed by Mitsuguchi et al. (1996) and some recent success has been shown in the Mediterranean coral *C. caespitosa* pertinent to this study (Montagna et al., 2007).

1.3 Clumped Isotopes

Although Sr/Ca improves on $\delta^{18}O$ in corals as a temperature proxy, the ideal paleothermometer would be entirely independent of seawater chemistry, thereby providing an absolute control on temperature without the need for assumptions of past cation concentrations or $\delta^{18}O_{seawater}$. One option is carbonate clumped isotope thermometry, a relatively new proxy that does not require assumptions about the isotopic composition of seawater. Clumped isotope thermometry measures a property of carbonate that is in theory purely thermodynamically determined provided the carbonate precipitation occurred under equilibrium conditions (Ghosh et al., 2006; Eiler 2011). The technique can be applied to either biogenic carbonates (e.g. shells and

skeletons of foraminifera, bivalves, corals, etc.) or abiogenic systems (e.g. paleosols, lake sediments, or speleothems).

In general, the term 'clumped isotopes' refer to any two heavy (and therefore typically rare) isotopes clumped together in a chemical bond. In the simplest case of diatomic hydrogen with a given concentration of deuterium isotopes, the system contains primarily three isotopologues: H_2, HD, and D_2. Bonds with one heavy isotope have a lower vibrational energy than bonds with only lighter isotopes, making them slightly stronger. By extension, 'clumped' bonds that contain two heavy isotopes are stronger still. Given a specific abundance of D (δD) one could calculate the expected stochastic distribution of D-D bonds. However in hydrogen and most other clumped isotope systems the measured abundance is enriched relative to this prediction by a factor defined as Δ_i for isotopologue i which was found to be inversely proportional to temperature (Wang et al., 2004; Ghosh et al., 2006; Eiler 2011).

Carbonate clumped isotope thermometry, reported as Δ_{47}, measures the abundance of the $C_{13}O_{18}O_{16}$ isotopologue (molecular mass 47) relative to all other isotopologues as a ratio against the stochastically expected distribution of heavy isotope clumping. This stochastic distribution is calculated from the abundance of the individual isotopes, described in detail by Affek and Eiler (2006). Positive values of Δ_{47} mean the carbonate has more heavy isotope clumping than would be expected if bonds were random. The thermodynamic preference of heavy isotopes to bind to each other is more pronounced at lower temperatures, so Δ_{47} is inversely proportional to temperature (Ghosh et al., 2006; Eiler 2011).

The first calibration curve for the proxy was built from inorganic calcite precipitation experiments carried out at temperatures from 1 to 50 °C (Ghosh et al., 2006). A diverse suite of

biogenic aragonites and calcites have since been shown to align well with this curve (Tripati et al., 2010; Zaarur et al., 2011; Thiagarajan et al., 2011; Eiler, 2011). These studies lend credence to the claim that the Δ_{47} proxy is not vulnerable to biological effects. In both bulk corals (Ghosh et al., 2006) and Indonesian and Red Sea *Porites* hermatypic corals, Δ_{47}-derived temperatures were within 1.5 °C of estimated growth temperatures (Ghosh et al., 2006; Thiagarajan et al., 2011). However, these applications of the Δ_{47} proxy to corals were mainly annual signals and little work has been performed at sub-annual resolution, likely due to the material-intensive nature of the analytical work (3.5 mg/replicate, 3-4 replicates per sample). Saenger et al. (2012) analyzed an assemblage of symbiotic, asymbiotic, hermatypic, and ahermatypic corals shallow-water corals with some sub-annual measurements. Two *Porites* corals were consistently offset toward higher Δ_{47} yielding temperatures underestimated of ~8 °C, the proposed explanation being that higher calcification rates are linked with increased kinetic offset (Saenger et al., 2012). With this potential challenge to interpreting Δ_{47} as SST in mind, this study applies carbonate clumped isotope thermometry to a shallow-water Mediterranean coral for the first time, focusing on sub-annual variability.

1.4 Magnesium isotopes

Recent advances in analytical precision have allowed the measurement of not just concentrations of trace elements, but the actual isotopic ratios of many alkaline earth elements including Mg^{2+}, Ca^{2+}, and Sr^{2+}. As Mg^{2+} is incorporated into aragonite from seawater, isotopic fractionation occurs in the form $\Delta^{26}Mg = \delta^{26}Mg_{aragonite} - \delta^{26}Mg_{seawater} \approx 1000\ln\alpha$, where α is the fractionation factor (Wang et al., 2013a). Recent work has demonstrated the temperature

dependence of this fractionation in the Mg isotope system at ~0.01‰ per °C through abiogenic aragonite precipitation experiments (Wang et al., 2013b). Saenger et al. (2013) found an unexpectedly large fractionation factor of ~0.3 ‰ per °C in *Porities* corals indicating that while an empirical calibration is possible and worth pursuing, vital effects appear to be important as well in affecting Mg isotope fractionation.

2. Biology and geochemistry of *Cladocora caespitosa*

Paleothermometry using corals in the Mediterranean has focused on the scleractinian zooxanthellate coral *Cladocora caespitosa* (L.), one of the major carbonate producers in the Mediterranean both in recent and past times (Peirano et. al., 2001). *C. caespitosa* is the only extant, endemic colonial coral in the Mediterranean and has been dominant since the early Pleistocene (~2.5 Ma) (Peirano et al., 1999). Colonies typically occur on sandy and rocky bottoms, preferring shallow depths of 4-10 m but persisting with less abundance from 10-40 m (Peirano et al., 2001; Kružić et al., 2008). This preference for shallow water means that *C. caespitosa* experience and therefore record the climate conditions of the upper thermocline which can be approximated by the parameters SST and SSS. *C. caespitosa* grows in distinct, hemispherical colonies that can rise up to 1 m above seafloor and cover several square meters area (Peirano et al., 2004), allowing multiple corallites from the same or adjacent colonies to be compared.

Linear growth rates exhibit ranges of 1.3-4.3 mm/year in the Ligurian Sea in the colder Western Mediterranean (Peirano et al., 1999) to 2.8-6.2 mm/year in some sites in the Southeastern Adriatic (Kružić and Požar-Domac 2003). This total annual extension is divided

between a high-density (HD) band deposited during the cold, rainy Mediterranean winter (November–March) and a low-density (LD) band deposited during the warm, dry summer season (July–September) (Peirano 1999; Peirano 2004). While the precise mechanism responsible for HD-LD band alternation is unknown, data suggests a correlation between LD band deposition and high light intensity and warm temperatures (Peirano et al., 1999). Stronger seasonal extremes in SST lead to more pronounced banding, though trace element ratio proxies have shown that *C. caespitosa* stops calcifying when seawater drops below 14 °C and becomes stressed around and above 23 °C (Montagna et al., 2007). This means that extremely cold temperatures are not recorded and extremely warm temperatures may be recorded with altered fidelity. If seasonal variation in SST is small with homogenously warm temperatures year round banding is absent entirely which would cause difficulty identifying individual years in some time periods (e.g. Eemian, 130 ka with temperatures 2-4 °C higher than today) (Van de Berg et al., 2011). *C. caespitosa* typically initiates the deposition of its HD band in November with a ring at the top of the septa. HD bands finish forming around March and constitute more linear extension than do the LD bands formed in the warm summer months (Peirano et al., 1999). One year of growth is typically defined from winter to winter as the distance between two successive HD density peaks (Peirano et al., 2004). Interestingly, Peirano et al. (1999) also showed that deep (>10 m) and shallow colonies contained nearly identical banding patterns despite lower ambient seawater temperatures for the deep specimens, lending credence to the theory that light intensity is more important than temperature in triggering that initiation of HD and LD band formation. Some *C. caespitosa* sampling methods use a diamond saw to cut the corallite at the LD band, thus eliminating it but preserving the HD band (Silenzi et al., 2005; Montagna et al., 2007). While this method causes some fidelity to be lost from the warmest part of the year, the missing portion

is small and reflects only a brief window on the warmest, most stressful conditions. Furthermore, the HD band is deposited when zooxanthellae activity is lowest making it potentially more resilient to vital effects (Silenzi et al., 2005). A *C. caespitosa* corallite was shown above in Figure 1 with HD and LD bands indicated.

Previous work assessed the use of $\delta^{18}O$ as a temperature proxy in *C. caespitosa* over annual cycles and found a poor relationship between $\delta^{18}O$ and SST, though a low but nevertheless significant regression coefficient was observed between $\delta^{18}O$ and Sr/Ca ($r = -0.51$) (Silenzi et al. 2005). Trace element ratio work has been more extensive. Both a long term record correlating Sr/Ca and Mg/Ca with SST (Silenzi et al. 2005) and a high-resolution time series of Sr/Ca, B/Ca, U/Ca, Mg/Ca, and Ba/Ca vs. SST (Montagna et al., 2007) have been performed on the species.

This study aims to improve understanding of $\delta^{18}O$ as a SST and SSS proxy in *C. caespitosa*, confirm the above mentioned calibrations of Sr/Ca and other trace element ratios, and use these proxies to constrain and characterize the behavior of clumped isotopes and Mg isotopes, the first time these new proxies have been applied to a shallow-water Mediterranean coral.

3. Materials and Methods

3.1 Study Area

For this study, specimens of *C. caespitosa* were collected from Mljet National Park, located on the island of Mljet, Croatia in the South Adriatic Sea (42°46'9"N, 17°22'27"E), 62 km west-northwest of the city of Dubrovnik. Figure 2 shows Mljet's location in the Adriatic as well as a close-up of the island's northwest tip including the seawater lakes Veliko Jezero and Malo Jezero.

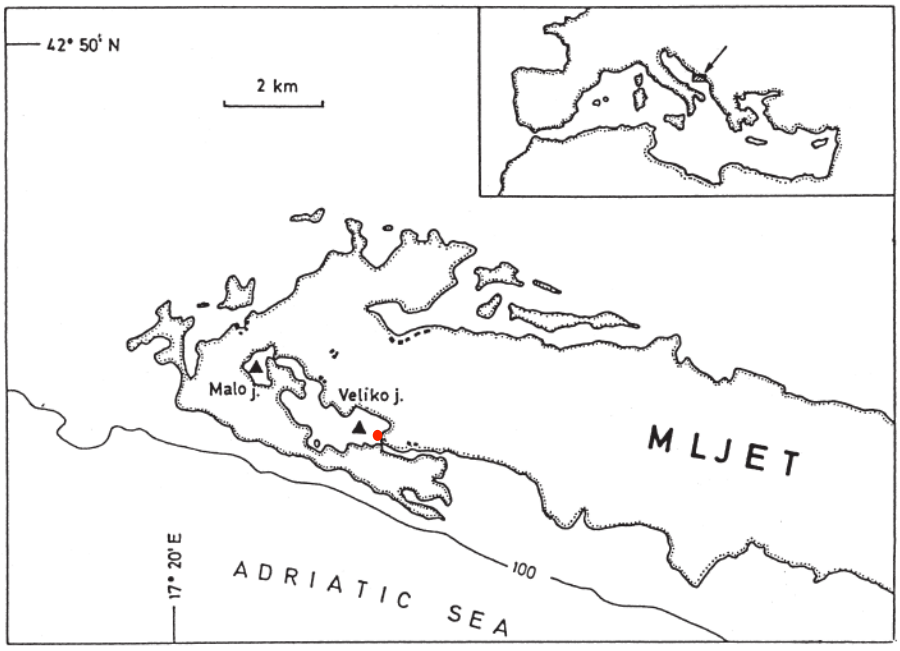

Figure 2 - Map of Mljet, Croatia detailing the seawater lakes Veliko Jezero and Malo Jezero. Black triangles indicate deepest locations within each lake (46 m and 29 m respectively). Red point indicates site where Cladocoa caespitosa specimens were collected. Map reproduced and modified from Benović et al. (2000).

The two seawater lakes are karstic depressions that formed 4,200 and 7,000 years B.P. respectively and are connected to the open sea by a channel at the southeast extreme of Veliko Jezero (Benović et al., 2000). The karstic saltwater lakes are home to one of the largest banks of *C. caespitosa* as well as to a diverse community of medusae (Benović et al., 2000; Kružić and Požar-Domac 2003). Temperatures can range from ~9.7 in February to 29 °C in August (Kružić and Požar-Domac 2003), well above the proposed ~23 °C threshold above which *C. caespitosa* begins to experience biological stress (Montagna et al., 2007). Indeed underwater photography taken

during field work in 2011 showed evidence of bleaching in some of the shallower *C. caespitosa*, a necessary consideration when employing the species for paleoclimate reconstruction (Kružić, unpublished). *C. caespitosa* colonies thrive in Veliko Jezero, benefiting from strong tidal exchange, and cover over 650 m^2 of the seafloor (Kružić and Požar-Domac 2003). Precipitation over this part of the Adriatic has an average $\delta^{18}O$ of - 5.43 ‰ (VSMOW, weighted average of annual time series from GNIP database) (IAEA/WMO 2006) which reflects the fact that strong evaporative flux in the Adriatic leads to highly depleted water vapour and subsequent precipitation (Rohling et al., 2009). This $\delta^{18}O_{precipitation}$ input has the potential to alter $\delta^{18}O_{sw}$, as does evaporative enrichment.

3.2 Environmental specimens

Corallite M-1 was collected on October 3rd, 2003 at 10 m depth by Dr. Simone Galeotti in Mljet, Croatia at the mouth of the large seawater lake Veliko Jezero. The specimen was preserved in formalin and transported to Yale for analysis in May, 2012. Additional corallites M-2, 3, and 4 were collected at 10 m depth from the same site on June 30th, 2011, along with seawater samples at 9.3 and 25 m depth. All corallites were photographed and corallite M-1 was scanned using a Scanco uCT-35 at 10 micron isometrix voxel size resolution to maintain a record of internal structure and density banding after destructive sub-sampling (see Figure 3).

A dremel at low speed was used to lightly abrade and clean the outer layer of corallite M-1. Using a hand file, corallite M-1 was subsampled into ~2-4 mg portions of finely ground aragonite powder. Filing was performed perpendicular to the growth axis to minimize mixing between adjacent samples. After each subsampling, the length of the corallite was measured to

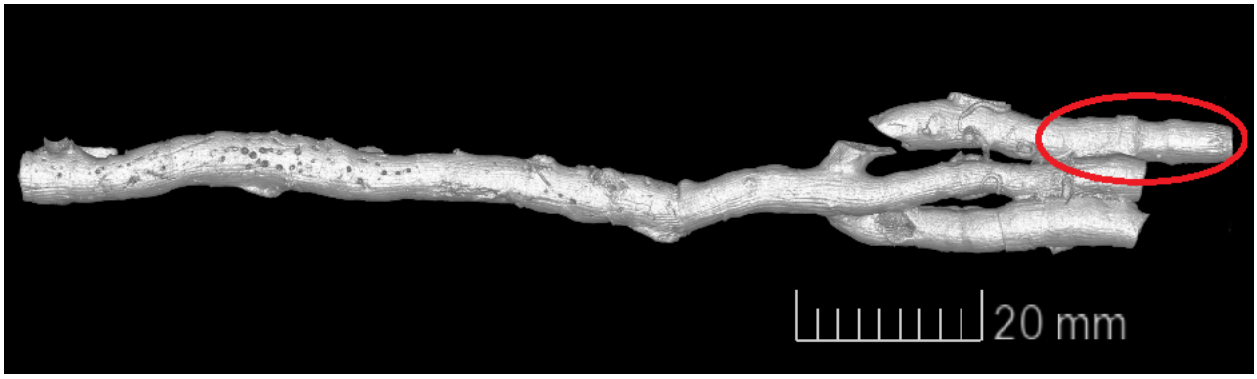

Figure 3 - Micro CT scan of corallite M-1 with sub-sampled area indicated in red.

provide a record of growth rate to associate with each subsample. Exterior annual bands and the CT scan were used together as a guide to separate one year of corallite growth from another. In total, 60 subsamples were collected representing 1.13 cm of linear extension and 211 mg of aragonite.

3.3 Aquaria-cultured corals

This study also analyzes material taken from colonies of *C. caespitosa* that were cultured in aquaria for a separate study. In 2006, three colonies of *C. caespitosa* were collected from the Gulf of La Spezia (Ligurian Sea, 44°03' N, 9°55' E) and acclimated for two weeks in aquaria at the Scientific Centre of Monaco (CSM). Following acclimatization, the corallites were randomly distributed among tanks maintained at 15, 18, 21, and 23°C and allowed to grow and calcify for 87 days. Fresh seawater was supplied at a rate of 2 L/hr. Alzarin Red S stain was used as a marker to indicate where new skeletal growth began. The specimens were measured for Mg/Ca and Sr/Ca (Montagna, unpublished) and additional aragonite was later recovered in July, 2011 by mechanically scouring above the stain line in July before being transported to Yale for additional

measurements. The aragonite samples were crushed into fine powders using mortar and pestle and prepared for clumped isotopes and magnesium isotopes analysis as detailed below.

3.4 Oxygen and carbon analytical methods

For each of the 60 subsamples, ~225 µg of aragonite was separated for analysis and placed in a centrifuge vial with a septa-sealed cap. The vials were flushed with ultra-high purity He to evacuate all air. Each sample was injected with 0.1 mL 105% phosphoric acid, centrifuged for 5 minutes, and allowed to react overnight at 25 °C. $\delta^{18}O$ and $\delta^{13}C$ values were then measured using a Delta-XP mass spectrometer at the Yale University Earth Systems Center for Stable Isotopic Studies. Two NBS-19 and two SECM standards were measured to correct the data, along with eight UTM standard replicates to account for drift and calculate standard error.

3.5 Clumped isotopes analytical methods

For samples whose $\delta^{18}O$ values were found to cluster around seasonal minima and maxima, ~2mg of the powder remaining to that sample was removed and combined with adjacent samples to yield five mixed samples of 15-20 mg each. These five combined samples were measured for Δ_{47}. 3-4 replicate Δ_{47} measurements were performed for each bulk sample to produce a statistically robust result.

The analytical protocol for clumped isotopes follows that reported in Zaruur et al. (2011) and Saenger et al. (2012). In brief, ~3.4-3.8 mg was digested for eight hours in 105% phosphoric acid at 25 °C. The CO_2 resulting from this digestion was cryogenically extracted and cleaned of

organic contaminants using a gas cromatograph column (Supelco Q-Plot, 30 m length, 0.53 mm ID) at – 20 °C. Once cleaned the CO_2 was measured using a Finnigan MAT-253 gas source isotope ratio mass spectrometer configured to measure masses 44 through 49 at the Yale University Earth Systems Center for Stable Isotopic Studies. The beam of interest at mass 47 consists primarily of the $^{13}C^{18}O^{16}O$ isotopologue and is used to calculate the ratio of mass 47 to mass 44 (R^{47}).

3.6. Trace metal analytical methods

From the original 60 subsamples, remaining material from adjacent samples was combined to yield 26 mixed subsamples (A-Z) of ~3 mg of material each. The material was weighed precisely and placed in acid-cleaned centrifuge tubes. Aragonite was washed and dissolved using a stepped leaching process. During each dissolution step, samples were ultrasonically cleaned for 10 minutes and centrifuged for 5 minutes. The solution from each non-H_2O step was collected and preserved for subsequent trace element measurements. The dissolution steps were performed in the following sequence: weak ammonium acetate (NH_4Ac), twice Milli-Q H_2O, 10% methanol (MeOH), twice Milli-Q H_2O, 0.1 % acetic acid (HAc) twice, 0.25 % HAc twice, and 1% HAc once.

For solutions from the second 0.1 % and first 0.25 % acetic acid steps, 0.8 mL of each sample was transferred into vials and set aside for column chemistry and magnesium isotope analysis. The remaining 0.2 mL was dried down, then dissolved in 3N nitric acid (HNO_3) and dried down again. Once dry, 3.8 mL of 5% HNO_3 doped with 2 ppb indium was added to each sample to prepare for trace element analysis. Samples were measured using a single collector

ICP-MS (Element XR) at Yale University. All measurements were made in medium resolution and compared against an in-house JAP coral standard at 0.2%, 0.5%, 1%, 2%, and 5%.

3.7 Magnesium isotope analytical methods

For each culture coral growth temperature (15, 18, 21, and 23 °C) two portions of 3 mg were measured out and placed in acid-cleaned centrifuge vials. The samples were subjected to a leaching procedure similar to that described above except the HAc steps were not stepped but rather a single dissolution using 1% HAc was performed and the solution collected

Due to the risk of isobaric interferences (e.g. $^{6}Li^{18}O^{+}$, $^{7}Li^{18}O^{+}$, $^{23}NaH^{+}$, and particularly $^{48}Ca^{2+}$) and matrix effects that can alter $\delta^{26}Mg$ results, all other cations (e.g. Na^{+}, Ca^{2+}, Sr^{2+} and Ba^{2+}) were carefully separated using two cation chromatographic columns as detailed by Wang et al. (2013a). Sample powders were dried down, dissolved in 6.2 N HCl, and dried down again. Next, each sample was dissolved in 250 μL of 2.5 N HCl. 200 μL was extracted for magnesium isotope analysis while the remaining 50 μL was reserved for trace metal analysis. For each sample the 200 μL of solution was dried down and 2.5 N HCl was added before drying the samples down again. Finally, 200 μL of 1.5 N HNO_3 was added to each sample before loading them onto Biorad cation resin AG50W-X12 (H^{+} form) in a 4.3 cm Teflon column (0.6 cm OD). Samples were eluted in 1.5 N HNO_3 to ensure separation of Mg^{2+} from Na^{+} and remaining Ca^{2+} (see Wang et al., 2013a). The collected solution was dried down before dissolving in 3 N HNO_3 with a drop of 10% H_2O_2 (to remove any remaining organic molecules) and drying down again. Finally, each sample was dissolved in 4 mL of 5% HNO_3 for isotopic analysis. These purified

magnesium solutions were then measured using a Multi-Collector ICP-MS (Neptune) at Yale University.

4. Results

4.1. Stable isotopes ($\delta^{18}O$ and $\delta^{13}C$)

$\delta^{18}O$ and $\delta^{13}C$ values are reported in Figure 4. An acid fractionation factor of 10.63 ‰ was used to convert $\delta^{18}O_{CO2}$ to $\delta^{18}O_{aragonite}$ following Kim et al. (2007b). The $\delta^{18}O$ record varies between – 3.52 and – 1.49 for a total variability of 2.03 and a mean value of – 2.64. The $\delta^{13}C$ record varies between – 5.50 and – 4.66 for a total variability of 0.85 and a mean value of – 5.13. Both isotopic measurements are given in ‰ relative to the Vienna Peedee Belemnite standard (VPDB). Samples constituting $\delta^{18}O$ minima and maxima that were grouped together into bulk samples are enclosed within circles in Figure 4.

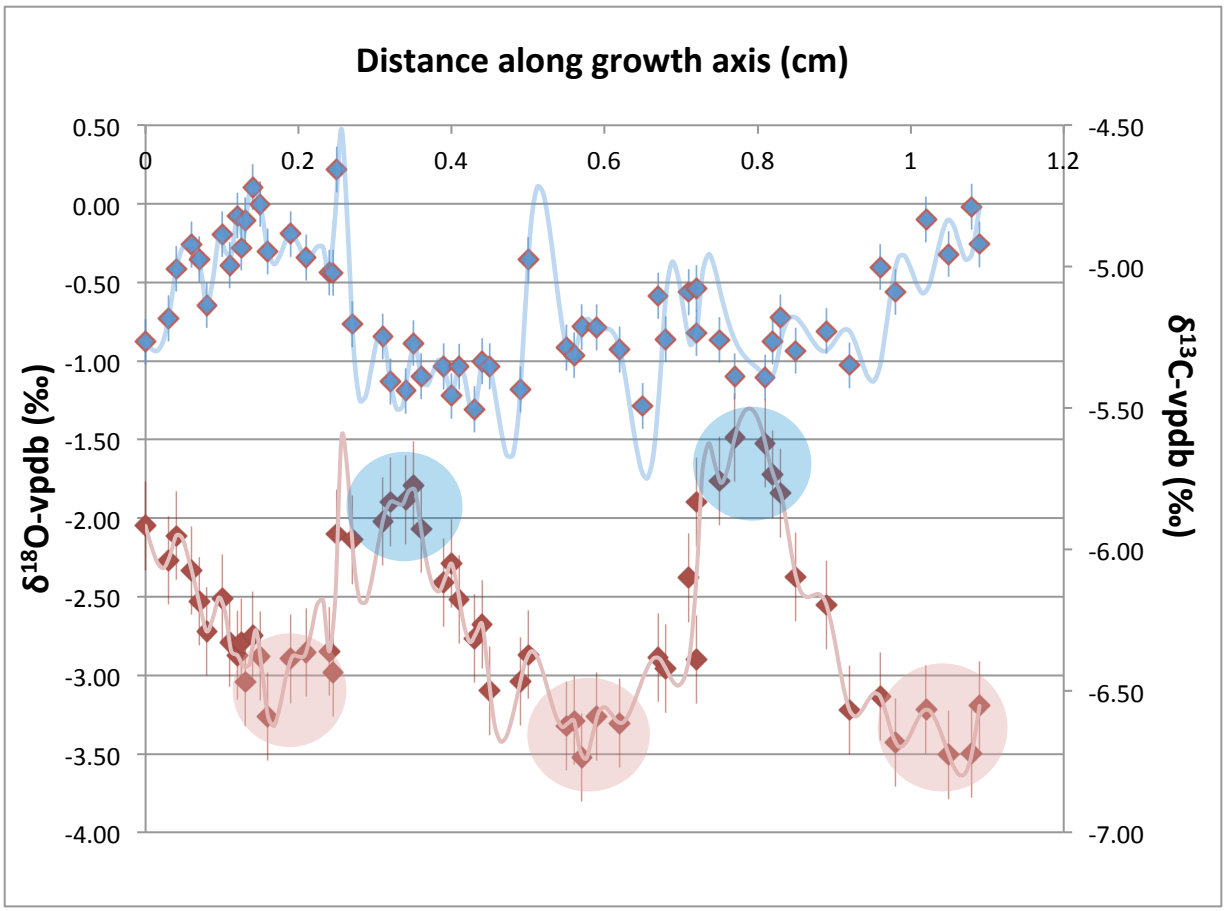

Figure 4 - $\delta^{18}O$ (red) and $\delta^{13}C$ (blue) values plotted against distance along growth axis. Red and blue lines are cubic spline interpolations of the $\delta^{18}O$ and $\delta^{13}C$ data respectively. Error bars represent 2 standard deviations. Circles indicate $\delta^{18}O$ minima and maxima. Samples within circles were grouped together for clumped isotope analysis.

4.2. Trace element ratios

Figures 5-9 show Na/Ca, Mg/Ca, Sr/Ca, U/Ca, and Ba/Ca ratios. Data include solution from both the second and third leaching steps combined on one plot. Blue lines are sixth order polynomial regressions. Y-axis error bars represent the absolute analytical error of the measurement while x-axis error bars reflect how many of the original 60 subsamples were mixed to form the data point.

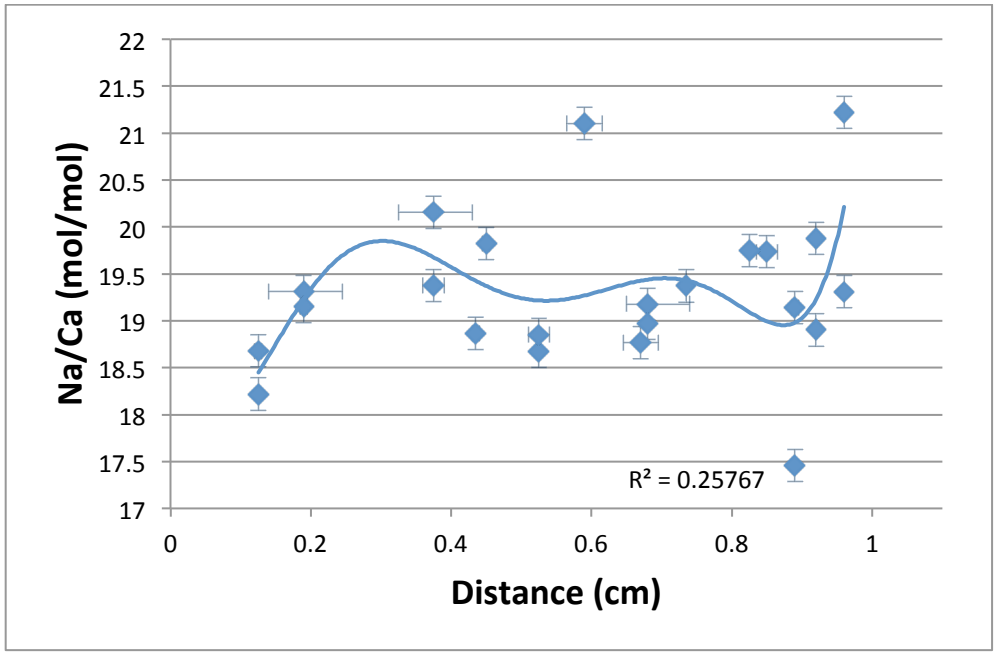
Na/Ca (mol/mol)
22
21.5
21
20.5
20
19.5
19
18.5
18
17.5
17
0
0.2
0.4
0.6
0.8
1
R² = 0.25767
Distance (cm)

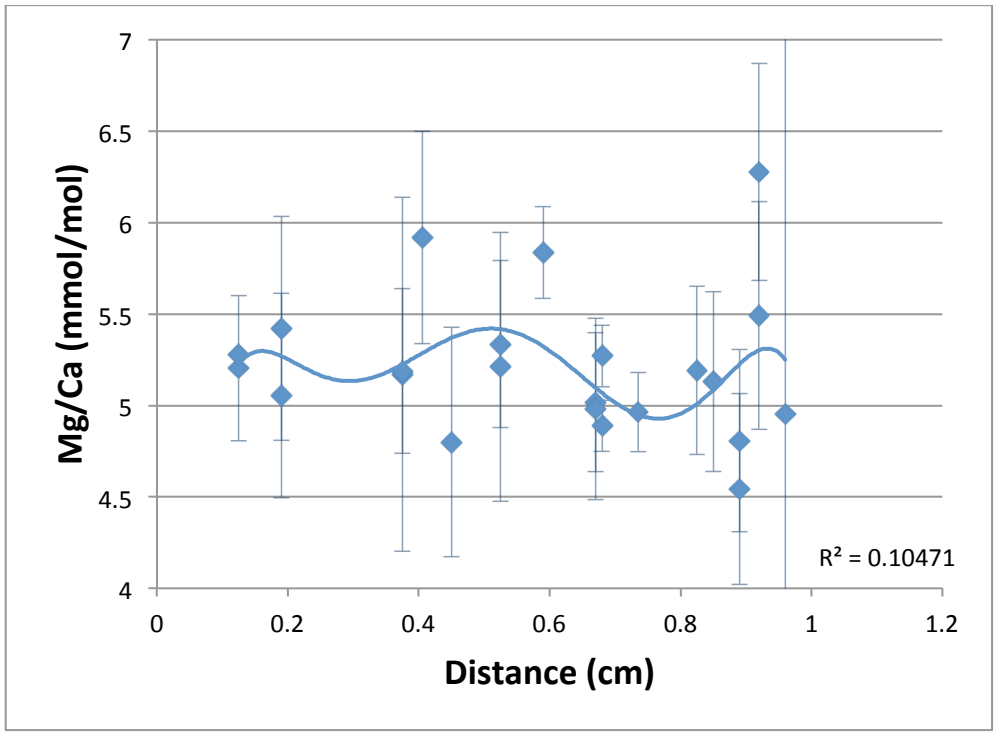
Mg/Ca (mmol/mol)
7
6.5
6
5.5
5
4.5
4
0
0.2
0.4
0.6
0.8
1
1.2
R² = 0.10471
Distance (cm)

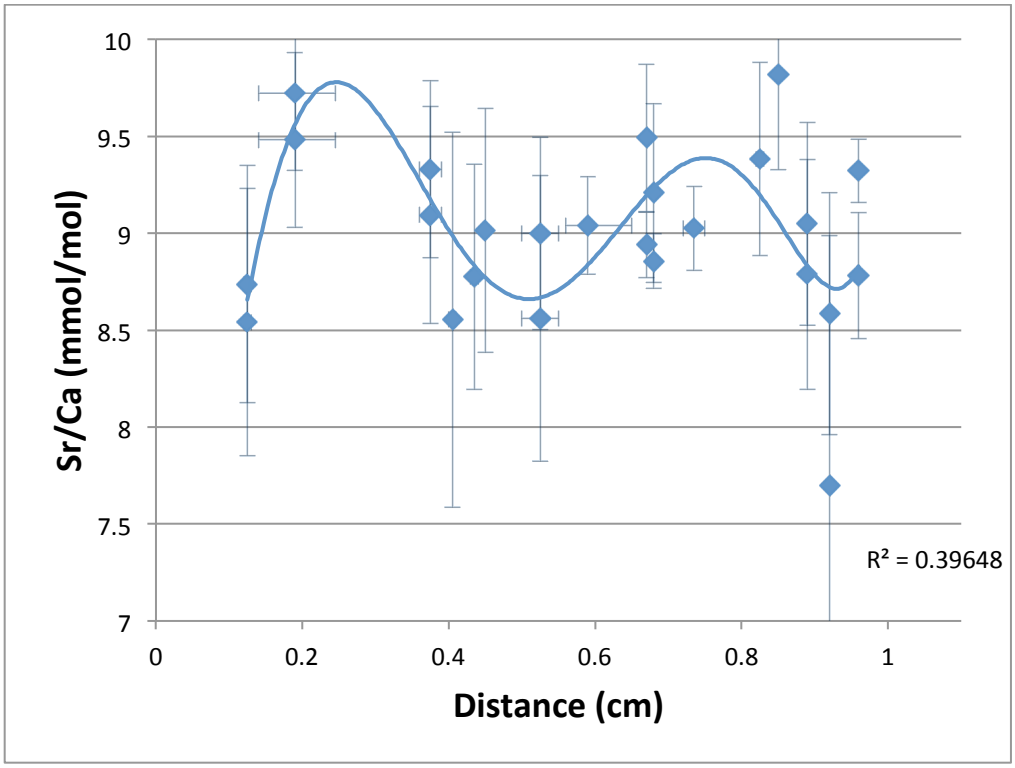
10
9.5
9
8.5
8
7.5
7
0
0.2
0.4
0.6
0.8
1
Sr/Ca (mmol/mol)
Distance (cm)
R² = 0.39648

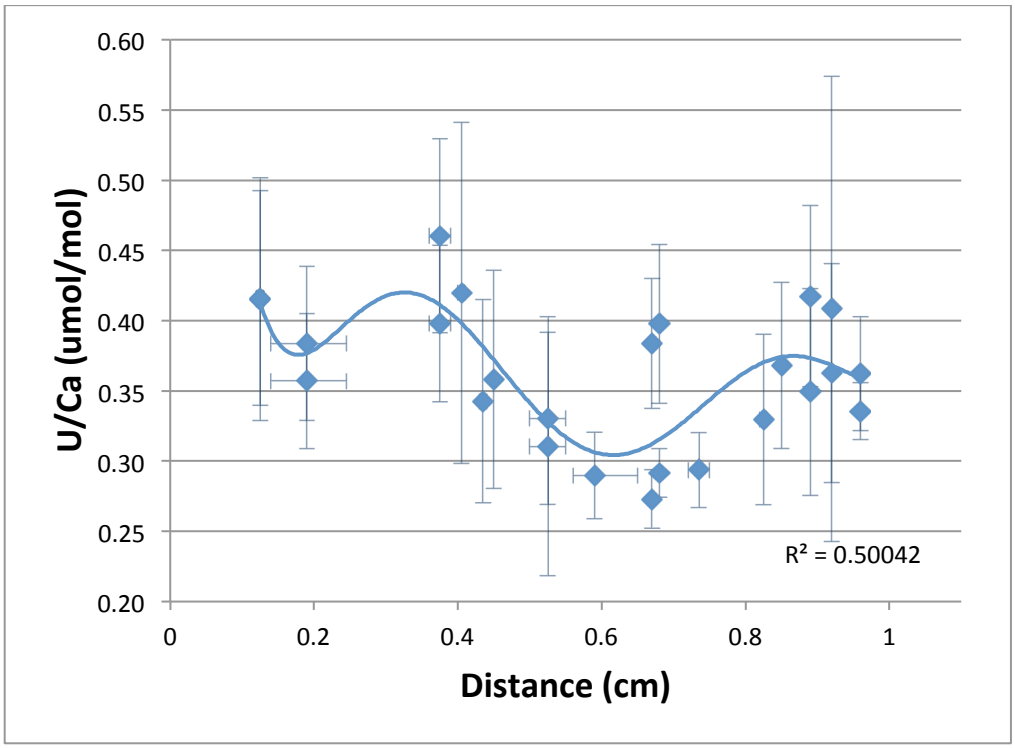
0.60
0.55
0.50
0.45
0.40
0.35
0.30
0.25
0.20
0
0.2
0.4
0.6
0.8
1
U/Ca (umol/mol)
Distance (cm)
R² = 0.50042

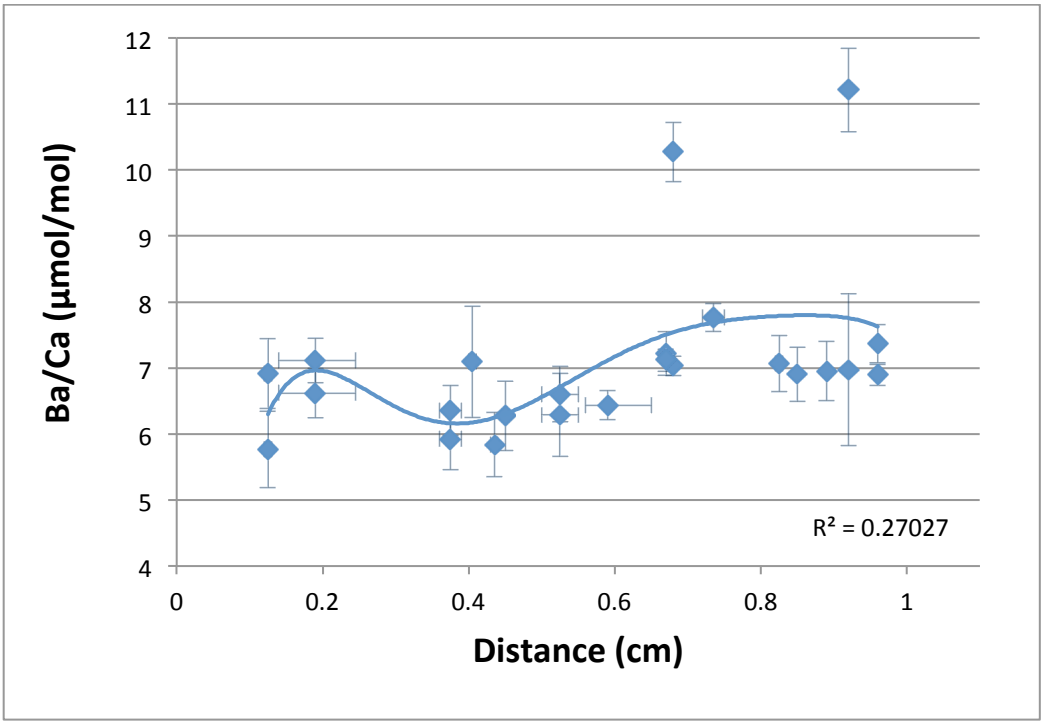

Figure 10 shows the percentage dissolved Mg^{2+} partitioned between the second and third leaching steps (0.1% HAc and 0.25% HAc respectively). This may indicate that $\delta^{26}Mg$ measurements should be performed on solution from leaching step two.

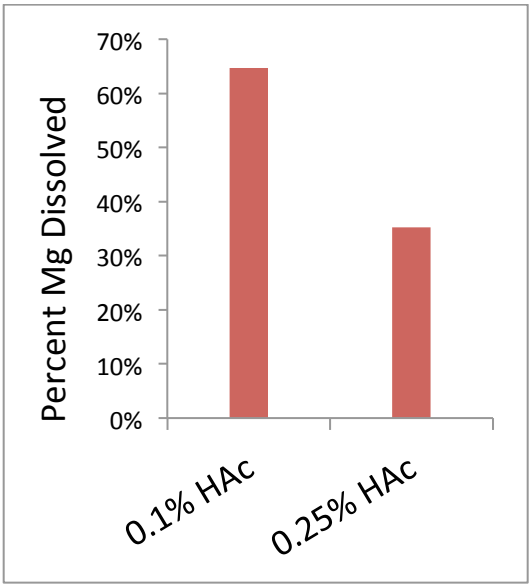

Figure 10 - Percent Mg^{2+} dissolved as partitioned between the second 0.1% and first 0.25% HAc dissolution steps.

4.3 Clumped Isotopes

Clumped isotope Δ_{47} values are summarized in Table 1 and Figure 11.

Table 1 - Clumped istotope data summary

Distance (cm)	1.05	0.77	0.58	0.335	0.175
$\delta^{13}C$	-4.791	-5.177	-5.225	-5.327	-4.842
$\delta^{18}O$ (sample)	38.057	39.732	38.098	39.560	38.603
$\delta^{18}O_{carbonate}$ (VPDB)	-3.7	-2.1	-3.7	-2.2	-3.2
Δ_{47}	-0.118	-0.113	-0.097	-0.126	-0.096
δ_{47}	11.680	12.970	11.626	12.533	12.193
Temp	16.2	16.0	11.2	18.9	11.5
Standard Deviation (Δ_{47})	0.012	0.020	0.021	0.011	0.019
Standard Error (Δ_{47})	0.00586	0.009906	0.010616	0.005313	0.009582

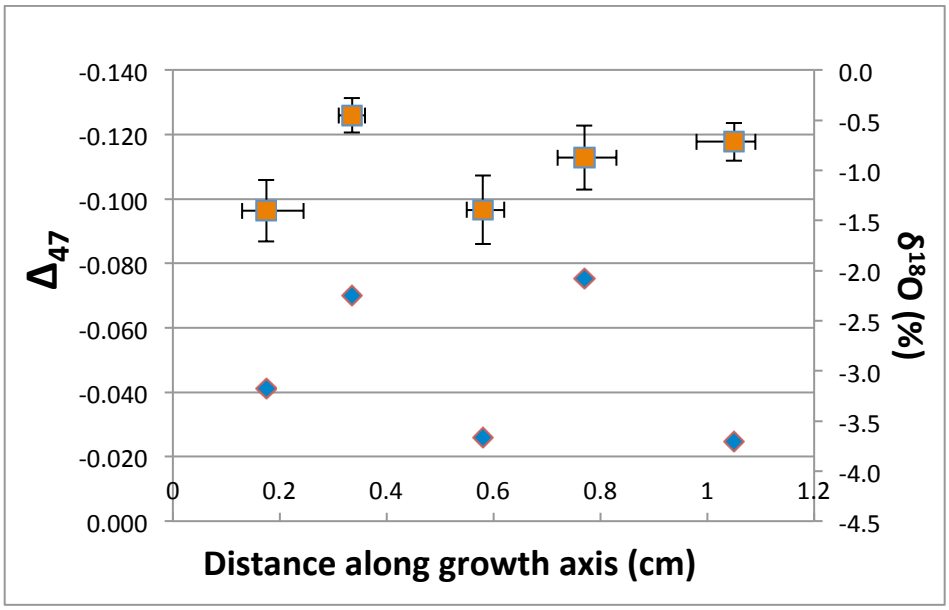

Figure 11 - Clumped isotopes values (orange) and d18O values (blue) measured on the dual inlet mass spectrometer. Error in the x-direction indicates length of the corallite across which the subsamples spanned before being mixed to form bulk samples.

5. Discussion

5.1. Oxygen isotope data

Oxygen isotope data shows clear seasonal cycles that are interpreted as reflecting seasonal cyclicity in SST. This is confirmed by Sr/Ca-derived temperatures presented below in the analysis of trace element ratio data. The colony was collected on October 3rd, 2003 when SST had yet to descend significantly from summer highs (e.g. 21.2 °C in September, 2003). However, the $\delta^{18}O$ record ends with a descent into winter (increasingly more positive $\delta^{18}O$ values). Given the delicate nature of the freshly grown septa surrounding the polyp it is likely that the most recently calcified material when the organism was collected was lost. This lost material corresponds with the very end of the last HD band and the beginning of the last LD band (~early March to October 3rd, 2013).

The seawater $\delta^{18}O$ (hereafter $\delta^{18}O_{sw}$) collected on site in June, 2011 was 1.48 ‰ at 9.3 m and 1.70 ‰ at 25 m depth (vs. VSMOW). This falls within the range of 1.30 to 1.69 ‰ range of surface $\delta^{18}O_{sw}$ variability in the southern Adriatic shown in previous work (Stenni et al. 1995). Assuming a constant $\delta^{18}O_{sw}$ of 1.48 ‰, $\delta^{18}O$-derived temperatures were calculated according to the Grossman and Ku (1986) equation for aragonite:

$$T\ (°C) = 20.6 - 4.34 * (\delta^{18}O_{aragonite} - \delta^{18}O_{sw})$$

Figure 11 shows these $\delta^{18}O$-derived temperatures and the instrumental temperature record (Grbec and Morović, unpublished; IAEA/WMO 2006) interpolated using a cubic spline. While there is clear correspondence in the timing of seasonal cyclicity between observed SST and $\delta^{18}O$-derived temperatures, $\delta^{18}O$ severely overestimates temperature and doesn't capture the full ~17 °C amplitude seen in the instrumental temperature record.

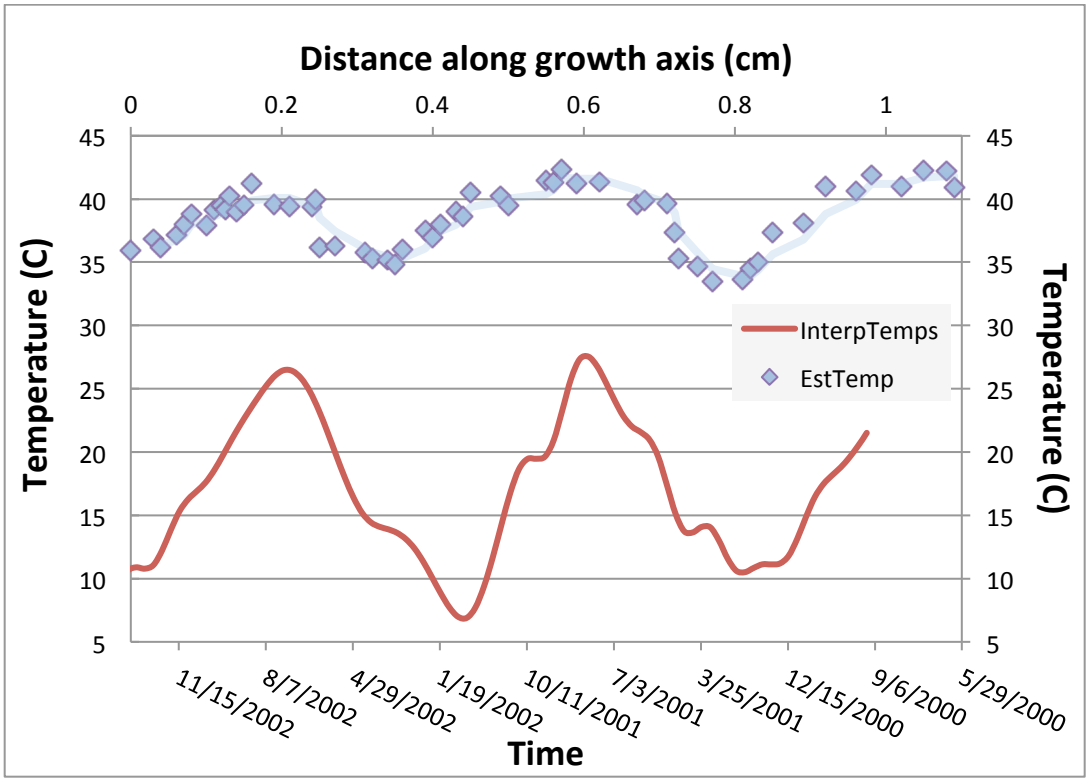

Figure 12 - instrumental temperature record (red) and d18O-predicted temperature (blue) plotted against time and distance along corallite respectively.

Given the large variability of salinity measured at 10 m depth in Veliko Jezero (~1 psu) it is likely that the observed $\delta^{18}O$ variability in corallite M-1 is influenced by both SST and changes in the isotopic composition of the ambient seawater (as reflected by SSS). While no *in situ* time series of $\delta^{18}O_{sw}$ exists, one can estimate the kinds of changes to surface isotopic composition that occur on an annual basis. A $\delta^{18}O_{precipitation}$ of -5.43 ‰ (VSMOW) was calculated using data from the Global Network of Isotopes in Precipitation (GNIP) database (IAEA/WMO 2006). Monthly $\delta^{18}O_{precipitation}$ averages from the Dubrovnik, Croatia station were weighted using average monthly precipitation values to reflect the actual volume of depleted precipitation added to the hydrologic system. Given the close proximity of the Veliko Jezero site to Dubrovnik (62 km) and the low altitude of both the Dubrovnik station and Veliko Jezero, this value should

reflect very closely the composition of precipitation experienced on Mljet. This isotopically light precipitation combined with fresh water river influx should lead to more negative $\delta^{18}O_{sw}$ values. Stenni et al. (1995) suggest that strong stratification in the Adriatic in Spring and Summer create a $\delta^{18}O_{sw}$ gradient with near 0 or even negative values at the surface that are not well mixed with water below. This study's measurement of $\delta^{18}O_{sw}$ at 25 m depth (1.70 ‰) suggests this stratification may be at play, but the values still show extreme enrichment, perhaps from a strong evaporative flux. Veliko Jezero exchanges water not only via tide-driven currents through the connecting channel but also through the karstic subsurface, another direct connection with Adriatic waters.

5.2 Trace element ratios

Analytical error was high for all trace metal measurements and the results from 24 samples were summarily rejected for having relative errors that exceeded the magnitude of some measurements. This is likely due to the fact that the trace element concentrations in these samples were very low, and the in-house JAP standard was only measured in standard concentrations. Future analysis will use JAP standards diluted such that the mass spectrometer counts are more comparable between sample and standard. The 24 high-error samples constituted approximately half of all samples measured and were evenly distributed between the second and third acetic acid leaching steps. The remaining samples with acceptable errors were well distributed throughout the length of subsampled corallite M-1, allowing time series to be constructed.

Sr/Ca and Mg/Ca ratios were interpreted as temperature according to the Montagna et al. (2007) calibrations for *C. caespitosa*:

$$\text{Mg/Ca (mmol/mol)} = 1.66 + 0.121 * \text{SST(°C)} \qquad r = 0.566$$

$$\text{Sr/Ca (mmol/mol)} = 10.50 - 0.073 * \text{SST(°C)} \qquad r = -0.723$$

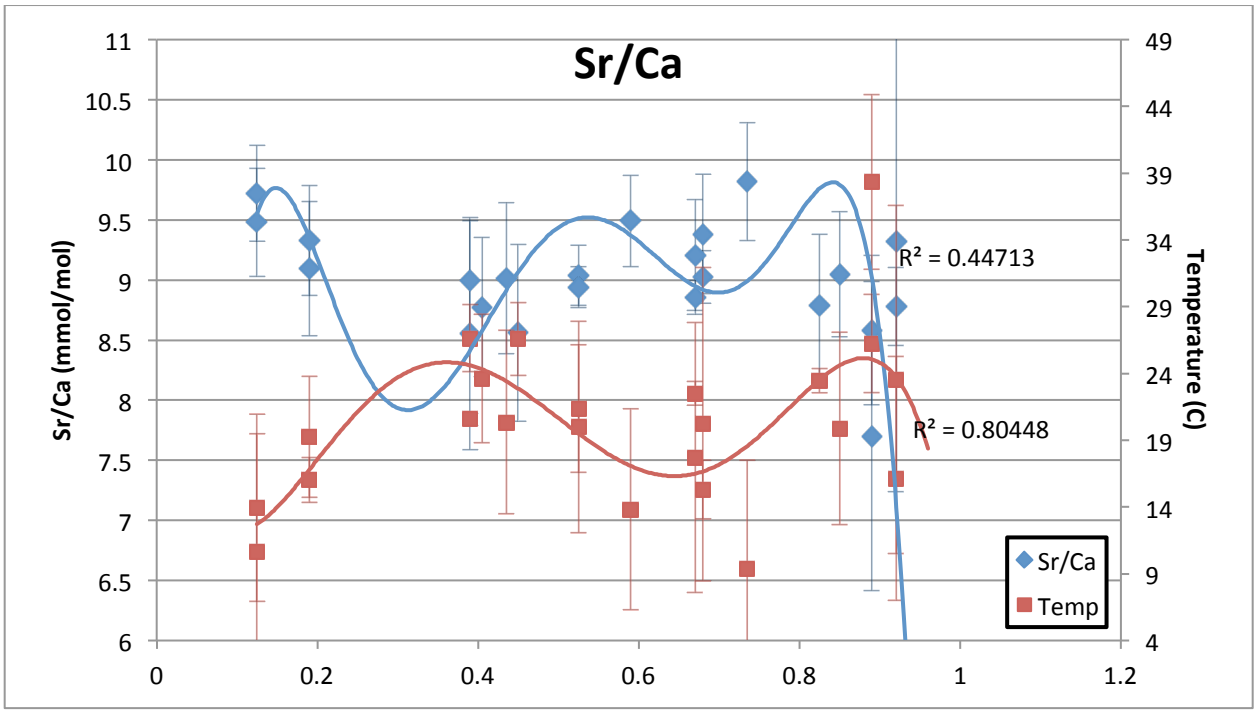

Figure 13 - Sr/Ca ratios are shown in blue for samples with acceptable relative error. Equivalent temperatures according to the Montagna et al. calibration (2007) are plotted in red with error bars.

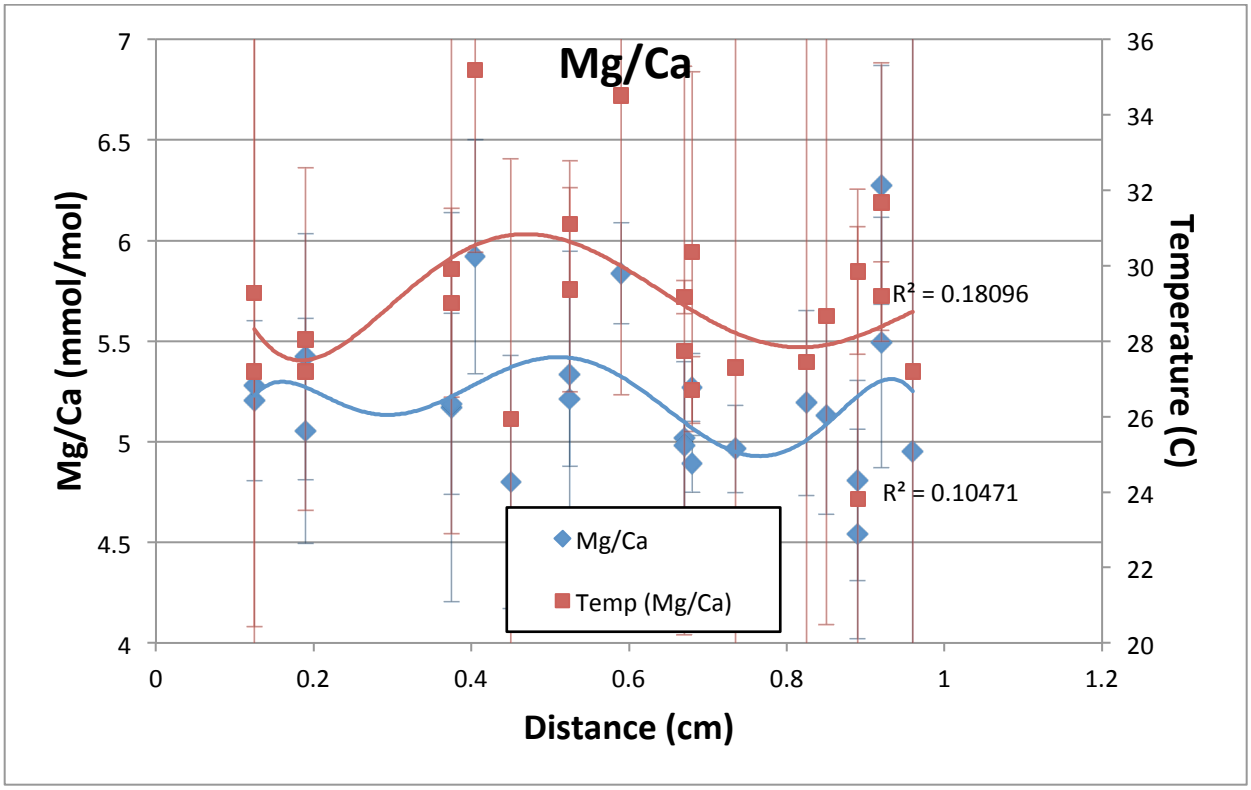

Figure 14 - Mg/Ca ratios are shown in blue for samples with acceptable relative error. Equivalent temperatures according to the Montagna et al. calibration (2007) are plotted in red with error bars.

Figure 13 shows Sr/Ca-derived temperatures which fall within the expected range of variability for the Veliko Jezero site showing lows of ~10 °C and highs of ~26 °C. Mg/Ca-derived temperatures (Figure 14) are overestimated, likely the result of the extreme analytical error. Additional analysis of concentrations will be attempted shortly with measures to greatly reduce analytical error and allow the meaningful interpretation of this data.

5.3 Comparing instrumental and proxy-derived temperatures

Temperatures derived from $\delta^{18}O$, Sr/Ca, and Δ_{47} are shown together with the interpolated instrumental temperature record in Figure 15. The extremely low Sr/Ca-derived temperatures in

the late Spring/early Summer of 2002 are likely an artifact from the high error and variability which is magnified by the cubic spline interpolation.

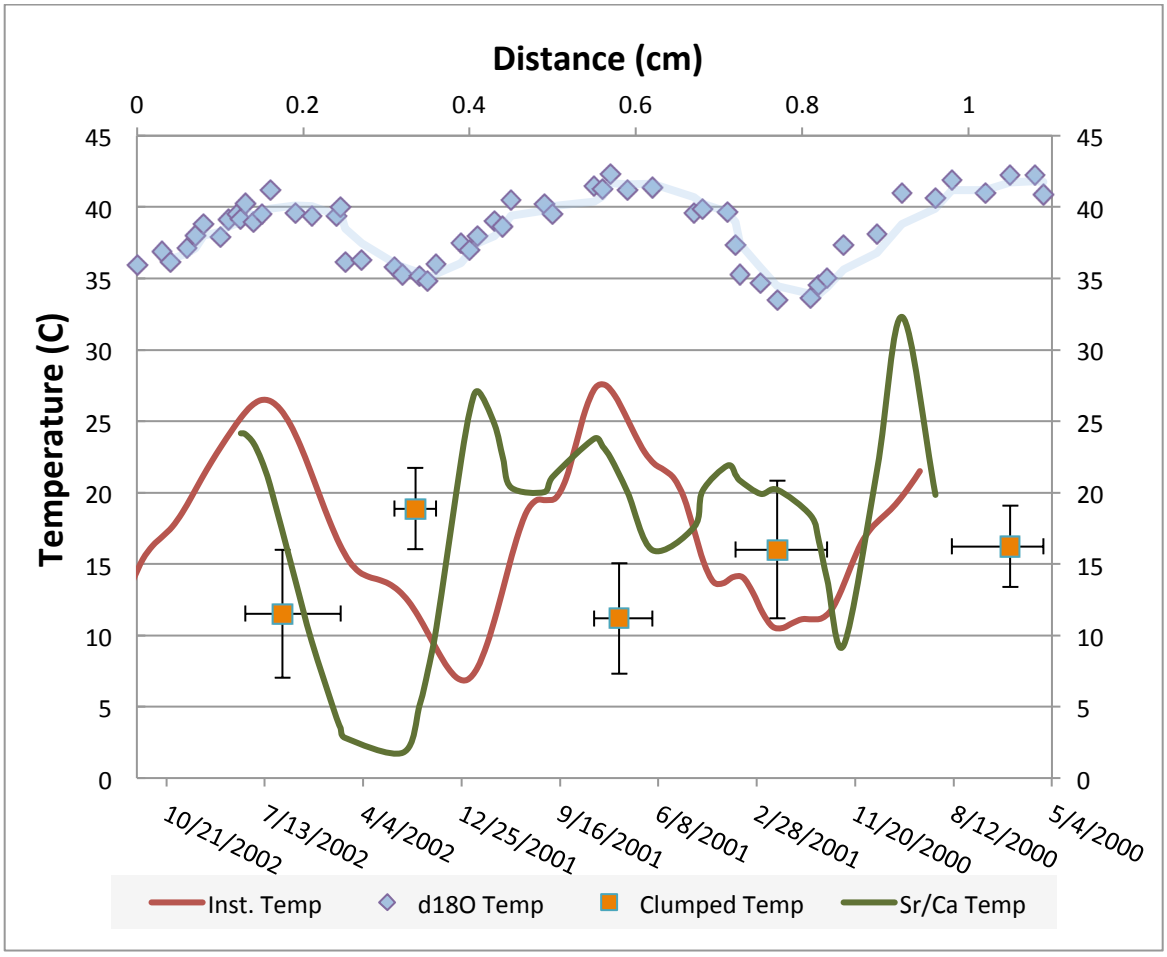

The temperatures derived from clumped isotopes are out of phase with other proxies, a surprising result considering the evidence for the lack of influence of biological vital effects on Δ_{47}. The most obvious explanation is that heterogeneities in mixed powder led to a low reproducibility of replicates. Additional replicates would reduce error if more material were available, but given the often wide range of Δ_{47}-generated temperatures among replicates of a single sample (reviewed above in Table 1), the effect would not be enough to shift temperature cyclicity making 'warm points' cold and vice versa. The low reproducibility could also stem from the

presence of organic molecules of masses that interfere with the 47 beam. However the δ_{48}, Δ_{49}, and $\Delta_{49/44}$ values, typically measured in order to screen for hydrocarbon contamination, were within acceptable limits.

6. Conclusions

This multi-proxy analysis of *C. caespitosa* confirms that it is possible to use this species to reconstruct sub-annual climate variability in the Mediterranean. Although the clumped isotope temperatures were inconsistent with other temperature proxies, they fell within a realistic range of possible temperatures for the site. The fact that $\delta^{18}O_{aragonite}$ values are highly out of equilibrium suggest that a pH effect in the calcifying fluid may be at least partially responsible for $^{18}O/^{16}O$ depletion. When converted into temperature estimates the . Magnesium isotope variability was incoherent among the cultured coral samples, though this may be a function . Additional $\delta^{26}Mg$ measurements of environmental samples, ideally corresponding to seasonal peaks and troughs, will help determine if there is marked temperature dependence in the magnesium isotopic fractionation recorded by *C. caespitosa.*

C. caespitosa offers a promising record for paleoclimate reconstruction in the Mediterranean. While Sr/Ca may be ready to be applied to the past the behavior of $\delta^{18}O$ appears to be closely tied to local conditions and the ability of this species to alter pH within the calcifying fluid and may elude interpretation without some knowledge of past climate conditions. Clumped isotope thermometry in *C. caespitosa* remains at a calibration stage and potential problems such as contamination by organics or heterogeneities in mixed samples must be

explored. The magnesium isotope measurements were inconclusive, showing no discernible pattern among the four samples grown at different constant temperatures in aquaria.

Acknowledgments

I would like to express my gratitude to Mark Pagani, Hagit Affek, and Zhengrong Wang for their guidance and support throughout the project. In addition, I benefited greatly from the ideas and assistance of Simone Galeotti, Paolo Montagna, Casey Saenger, Chao Liu, Glendon Hunsinger, Petar Kružić, and all of the students in the Affek and Pagani lab groups. I also thank the Von Damm and Alan S. Tetelman Fellowships for their generous support of this research.

References Cited

Artegiani, A. et al. 1997. *The Adriatic Sea General Circulation. Part I: Air–Sea Interactions and Water Mass Structure*. Journal of Physical Oceanography 27, 1492–1514.

Beck J. W., Edwards R. L., Ito E., Taylor F. W., Recy J., Rougerie F., Joannot P. and Henin C. (1992). Sea-surface temperature from coral skeletal strontium/calcium ratios. *Science* 257, p.644.

Benović A. Lučić D., Onofri V., Peharda M., Carić M., Jasprica N., and Bobanović-Ćolić. (2000) Ecological characteristics of the Mljet Islands seawater lakes (South Adriatic Sea) with special reference to their resident populations of medusa. *Scientia Marina* **64**, 197-206.

Billups, K, and Schrag, D. P. (2002) Paleotemperatures and ice volume of the past 27 Myr revisited with paired Mg/Ca and $^{18}O/^{16}O$ measurements on benthic foraminifera. *Paleoceanography* 17, 3-11.

Bethoux, J.P., Gentili, B., Morin, P., Nocolas, E., Pierre, C., and Ruiz-Pino, D. (1999) The Mediterranean Sea: a miniature ocean for climatic and environmental studies and key for a climatic functioning of the north Atlantic. *Progress in Oceanography* **44**, 131-146.

Bolle, H. et al. 2003. *Mediterranean Climate: Variability and Trends*. Springer, Berlin.

Burr G., Beck J., Taylor F., Recy J., Edwards R., Cabioch G., Correge T., Donahue, D., and O'Malley, J. (1998). A high resolution radiocarbon calibration between 11.700 and 12.400 calendar years BP derived from 230Th ages of corals from Espiritu Santo Island, Vanuatu. *Radiocarbon* **40**, 1093– 1105.

Cacho I., Grimalta J., Sierro F., Shackleton N., and Canals N. (2000) Evidence for enhanced Mediterranean thermohaline circulation during rapid climatic coolings. *Earth and Planetary Science Letters* **183**, 417-429.

Cohen A. L., Owens K. E., Layne G. D., and Shimizu N. (2002) The Effect of Algal Symbionts on the Accuracy of Sr/Ca Paleotemperatures from Coral. *Science* **296**, 331-333.

Correge, T. (2005). Sea surface temperature and salinity reconstruction from coral geochemical tracers. *Paleogeography, Paleoclimatology, Paleoecology* **232**, 408-428.

Craig, Harmon (1961) Isotopic Variations in Meteoric Waters. *Science* **26**, 1702-1703.

de Villiers S., Shen G., Nelson B. (1994). The Sr/Ca–temperature relationship in coralline aragonite: influence of variability in (Sr/Ca)seawater and skeletal growth parameters. *Geochimica et Cosmochimica Acta* **58**, 197– 208.

Eiler J.M. (2011) Paleoclimate reconstruction using carbonate clumped isotope thermometry. *Quaternary Science Reviews* **30**, 3575-3588.

Emiliani, C., Hudson, J., Shinn, E. A., George, R. Y., and Lidz, B. (1978) Oxygen and Carbon Isotopic Growth Record in a Reef Coral from the Florida Keys and a Deep-Sea Coral from Blake Plateau. *Science* 202, 627-629.

Epstein S., Ehhalt E. and Vogel J. (1951) Carbonate isotope fractionation during the precipitation of calcium carbonate. *Earth Planet. Sci. Lett.* **8**, 363-371.

Epstein S., Buchsbaum R., Lowenstam H. A. and Urey H. C. (1953) Revised carbonate water isotopic temperature scale. *Geological Society of America Bulletin* **64**,1315–1326.

Ghosh P., Eiler J., Campana S. E. and Feeny, R. F. (2006) Calibration of the carbonate 'clumped isotope' paleothermometer for otoliths. *Geochimica et Cosmochimica Acta* **71**, 2736-2744.

Grossman E. L. and Ku T. L. (1986) Oxygen and carbon isotope fractionation in biogenic aragonite: temperature effects. *Chemical Geology* **59**, 59–74.

Grottoli, A. (2001) Climate: Past Climate from Corals. In: Encyclopedia of Ocean Sciences. Eds Steele J., Thorpe S., and Turekian K. 2098-2107.

IAEA/WMO (2006). Global Network of Isotopes in Precipitation. The GNIP Database. Accessible at: http://www.iaea.org/water.

Keith, M. L., and Weber, J. N. (1965) Systematic Relationships between Carbon and Oxygen Isotopes in Carbonates Deposited by Modern Corals and Algae. *Science* **150**, 498-501.

Kim S.T., O'Neil J., Hillaire-Marcel C., and Mucci A. (2007a). Oxygen isotope fractionation between synthetic aragonite and water: Influence of temperature and Mg2+ concentration. *Geochimica et Cosmochimica Acta* **71**, 4704-4715.

Kim S.-T., Mucci A. and Taylor B. E. (2007b). Phosphoric acid fractionation factors for calcite and aragonite between 25 and 75 °C: revisited. *Chemical Geology* **246**, 135–146.

Kružić P. and Požar-Domac A. (2003). Banks of the coral Cladocora caespitosa (Anthozoa, Scleractinia) in the Adriatic Sea. *Coral Reefs* **22**, 536.

Kružić P., Žuljević A., and Nikolić V. (2008). Spawning of the colonial coral Cladocora caespitosa (Anthozoa, Scleractinia) in the Southern Adriatic Sea. *Coral Reefs* **27**, 337-341.

Lambeck K., Antonioli F., Purcell A., and Silenzi S. (2004). Sea-level change along the Italian coast for the past 10,000 yr. *Quaternary Science Reviews* **23**, 1567-1598.

McConnaughey, T. (1989a) ^{13}C and ^{18}O isotopic disequilibrium in biological carbonates: I. Patterns. *Geochemica et Cosmochimica Acta* **53**, 151-162.

McConnaughey, T. (1989b) ^{13}C and ^{18}O isotopic disequilibrium in biological carbonates: II. In Vitro simulation of kinetic isotope effects. *Geochemica et Cosmochimica Acta* **53**, 163-171.

McIntire, W. (1963). Trace element partition coefficients—a review of theory and applications to geology. *Geochemica et Cosmochimca Acta* **27**, 1209-1264.

Mitsuguchi T., Matsumoto E., Abe O., Uchida T., and Isdale P. (1996). Mg/Ca Thermometry in Coral Skeletons. *Science* **274**, 961-963.

Montagna, P. (2006) Li/Ca ratios in the Mediterranean non-tropical coral *Cladocora caespitosa* as a potential paleothermomer. *Geophysical Research Abstracts* **8**.

Peirano A., Morri C., and Bianchi N. (1999). Skeleton growth and density pattern of the temperate, zooxanthellate scleractinian *Cladocora caespitosa* from the Ligurian Sea (NW Mediterranean). *Marine Ecology Progress Series* **185**, 195-201.

Peirano A., Morri C., Bianchi N., and Rodolfo-Metalpa R. (2001). Biomass, carbonate standing stock and production of the mediterranean coralCladocora caespitosa (L.). *Facies* **44**, 75-80.

Peirano A., Morri C., Bianchi N., Aguierre J., Antonioli F., Calzetta G., Carobene L., Mastronuzzi G., and Orru P. (2004). The Mediterranean coral Cladocora caespitosa: a proxy for past climate fluctuations? *Global and Planetary Change* **40**, 195-200.

Rohling E., Abu-Zeid R., Casford J., Hayes A., and Hoogakker B. (2009). The marine environment: Present and past, in: J. Woodward, (Ed), The physical geography of the Mediterranean, Oxford university press, Oxford, 33-67.

Saenger, C., Affek, H., Felis, T., Thiagarajan, N., Lough, J., and Holcomb, M. (2012). Carbonate clumped isotope variability in shallow water corals: Temperature dependence and growth-related vital effects. *Geochemica et Cosmochimica Acta* **99**, 224-242.

Stenni B., Nichetto P., Bregant D., Scarazzato P., and Longinelli A. (1995) The $\delta^{18}O$ signal of the northward flow of Mediterranean waters in the Adriatic Sea. *Oceanologica Acta* **18**, 319-328.

Thiagarajan N., Adkins J. and Eiler J. (2011). Carbonate clumped isotope thermometry of deep-sea corals and implications for vital effects. *Geochim. Cosmochim. Acta* **75**, 4416–4425.

Tripati A., Eagle R., Thiagarajan N., Gagnon A., Bauch H., Halloran P., and Eiler J. (2010). ^{13}C–^{18}O isotope signatures and 'clumped isotope' thermometry in foraminifera and coccoliths. *Geochim. Cosmochim. Acta* **74**, 5697–5717.

Urey H. C., Lowenstam H. A., Epstein S. and McKinney C. R. (1951) Measurement of Paleotemperatures and temperatures of the upper Cretaceous of England, Denmark, and the southeastern United States. *Bulletin of the Geological Society of America* **62**, 399-416.

Van de Berg W., van den Broeke M., Ettema J., van Meigaard E., and Kaspar F. (2011). Significant contribution of insolation to Eemian melting of the Greenland ice sheet. *Nature Geoscience* **4**, 679-683.

Wang Z., Schauble E. A. and Eiler, J. M. (2004) Equilibrium thermodynamics of multiply substituted isotopologues of molecular gases. *Geochimica et Cosmochimica Acta* **68**, 4779-4797.

Wang Z., Hu P., Gaetani G., Liu C., Saenger C., Cohen A. and Hart, S. (2013a). Experimental calibration of Mg isotope fractionation between aragonite and seawater. *Geochimica et Cosmochimica Acta* **102**, 113-123.

Wang Z., Gautani G., Liu C., and Cohen A. (2013b). Oxygen isotope fractionation between aragonite and seawater: developing a novel kinetic oxygen isotope fractionation model. *Geochimica et Cosmochimica Acta* in press.

Weber J. N. and Woodhead, P. M. J. (1972) Temperature dependence of oxygen-18 concentration in reef coral carbonates. *Journal of Geophysical Research* **77**, 463-473.

Zaarur S., Olack G. and Affek, H. P. (2011) Paleo-environmental implication of clumped isotopes in land snail shells. *Geochimica et Cosmochimica Acta* **75**, 6859-6869.